RESEARCH PAPER

TiO₂/Ni₂CuO₃ Nanocomposite as the Efficient Visible-Light Photocatalyst for Degradation of Methyl Orange

Mustafa Saade Shakir 1*, Ban Samary Atyah 2

- ¹ Market Research and Consumer Protection Center, University of Baghdad, Iraq
- ² Environmental Research Center, University of Technology, Iraq

ARTICLE INFO

Article History:

Received 15 June 2025 Accepted 26 September 2025 Published 01 October 2025

Keywords:

Methyl orange Nanocomposite Ni₂CuO₃ Photocatalyst TiO₂ Visible light

ABSTRACT

A nanocomposite of TiO, and Ni₂CuO, nanoparticles was synthesized using two different synthetic methods, namely coprecipitation and solgel reactions. It was confirmed that incorporating 4 wt% of Ni₂CuO₃ nanoparticles enhanced the visible-light sensitivity and narrowed the optical band gap to 2.65 eV. Also, photoluminescence (PL) spectroscopy revealed the improved charge separation in the nanocomposite compared to the pure TiO, sample. The photocatalytic activity of the synthesized nanocomposites was assessed for degradation of methyl orange (MO) under visible light irradiation. By illuminating during 150 min, the degradation level of MO approached 94.17% using TiO₂/4 wt%-Ni₂CuO₂ nanocomposite. In comparison, the nanocomposites containing 2 wt% and 6 wt% of Ni₂CuO₃ nanoparticles were able to degrade the MO solution by 51.14% and 82.37%, respectively. Optimization experiments demonstrated that the highest degradation efficiency was obtained using 0.05 g of the nanocomposite at a pH of around 5. Moreover, reusability tests exhibited that the TiO₂/4 wt%-Ni₂CuO₃ nanocomposite retained the excellent photocatalytic activity over six successive reaction cycles without significant loss of efficiency.

How to cite this article

Shakir M., Atyah B. TiO₂/Ni₂CuO₃ Nanocomposite as the Efficient Visible-Light Photocatalyst for Degradation of Methyl Orange. J Nanostruct, 2025; 15(4):2251-2259. DOI: 10.22052/JNS.2025.04.064

INTRODUCTION

In recent decades, a wide range of pollutants, such as pesticides, dyes, oil and chemicals, have been released into rivers and seas [1, 2]. As a result, incident of fatal diseases, including cancer, has increased, promoting public health authorities to search for effective solutions [3]. At the same time, these pollutants have severely damaged ecosystems, leading to the extinction of many species [4, 5].

Recently, environmentally-friendly processes have been emphasized for removing pollutants,

aiming to minimize the harmful impacts associated with the use of harsh chemical treatment methods [6, 7]. In this context, photocatalysis have received considerable attention due to its advantages, such as no needs for toxic reagents, producing low hazardous by-products, and utilizing renewable energy resource—light [8, 9]. However, common photocatalysts, including TiO₂ and ZnO, have limitations to harness the visible light, as they are activated by absorption of UV light—consisting only 5% of light spectrum [10]. Additionally, their efficiency is affected by fast recombination rate of

^{*} Corresponding Author Email: mustafaaldori85@gmail.com

the photo-generated electrons and holes, thereby reducing their effectiveness for practical uses [11].

To overcome these obstacles, many scientific communities are endeavoring to synthesize the visible-light sensitized photocatalysts [12]. There are several proposed approaches for enhancing the light absorption abilities of the common photocatalyst materials. In this regard, doping metal and non-metal ions have been reported that significantly increase the photoactivity of TiO, [13, 14]. Moreover, coupling two or more metal oxides can effectively reduce the recombination rate of the electrons and holes [15, 16]. It materializes with the electronic transitions between the different energy levels of the different coupled materials [17, 18]. For instance, it has been reported that electronic transitions between TiO, and WO, can enhance the charge separation and the photocatalytic activity [19]. Also, Zhang and coworkers, reported the robust visible light photoactivity for $TiO_{2}@Bi_{2}O_{3}@TiO_{2}$ [20]. Kumar et al. studied photocatalytic degradation of pollutant using CeO,-TiO,@CNT [21].

Considering the photocatalyst materials previously reported in literature, a mixed metal oxide nanocomposite of TiO₂ and Ni₂CuO₃ was synthesized. To this end, two different synthetic methods were used. The NiCuO₃ nanoparticles were synthesized through precipitation reaction. Then, varied amounts of the NiCuO₃ nanoparticles were embedded to TiO₂ using sol-gel method. The photocatalytic activity of the synthesized nanocomposite was investigated by degradation of methyl orange (MO) under visible light irradiation. Also, the photoactivity of the synthesized nanocomposite was carefully assessed under different experimental conditions.

MATERIALS AND METHODS

Coprecipitation synthesis of Ni₂CuO₃ (NCO) nanoparticles

The NCO nanoparticles were synthesized by simple coprecipitation method, as follows: specific amount (0.1 g) of polyethylene glycol (PEG 400) was dissolved into 100 mL of distilled water as a capping agent. Then, Ni(NO₃)₂.6H₂O (2.0 mmol) and Cu(NO₃)₂.3H₂O (1.0 mmol) were added and the solution was stirred for 30 min. After that, the pH of solution was adjusted to about 9 using adding NaOH (0.1 M) dropwise. The solution was further stirred for 1 h. Next, the solid was separated using centrifugation at 6000 rpm for 10

min and then washed several times using ethanol/water solution. Finally, the solid was dried in an oven at 100 °C overnight.

Sol-Gel synthesis of TiO, nanoparticles

First, 0.05 g of polypropylene glycol (PPG) was dissolved into absolute ethanol and then specific amount of tetrabutyl orthotitanate (TBOT) was added. The solution was stirred for more than 1 h. Next, the solution was heated in an oven at 60 °C to form a viscous gel, which then further heated in a furnace at 600 °C for 4 h to form pure and crystalline ${\rm TiO_2}$ powder.

TiO_/Ni_CuO_ (TiO_/NCO) nanocomposite

Different amounts of the as-synthesized nanoparticles were mixed to prepare TiO₂/NCO nanocomposite. For this purpose, NCO nanoparticles (2 wt%, 4 wt%, and 6 wt%) were dispersed into the TiO₂ sol solution, and the solution was vigorously stirred for 2 h. The solution was converted to a viscous gel by heating and subsequently calcined to synthesized TiO₂/NCO nanocomposite. The drying and calcination temperatures were the same as those described in Section 2.2. The TiO₂/CNO-2, TiO₂/CNO-4, and TiO₂/CNO-6 stand for the TiO₂/CNO nanocomposite containing different amounts of CNO nanoparticles 2 wt%, 4 wt%, and 6 wt%, respectively.

Photocatalytic experiments

The photocatalytic efficiency of the TiO₂/NCO nanocomposites was studied using degradation of methyl orange (MO) under visible light irradiation. For that, a constant concentration of MO solution (40 ppm) was subjected to photocatalysis using varying amounts (0.03, 0.05, 0.07 g) of the prepared nanocomposites containing different NCO nanoparticles loadings (2 wt%, 4 wt%, and 6 wt%).

In order to illumination, an Osram lamp (400 W) was used as the visible light source, and illuminating was performed from constant distance of 50 cm. Before starting the illumination, the solution was stirred for 30 min in the darkness to reach the adsorption/desorption equilibrium. After that, the photocatalysis was initiated and the degradation level of MO was monitored by measuring the adsorption of MO at maximum wavelength (465 nm) using UV/Vis spectrophotometer. The procedure was carried out every 30 min by collecting 1 mL of the

MO solution. The photocatalyst particles were separated using centrifugation at 700 rpm for 15 min.

The photocatalysis of MO solution was conducted under different experimental conditions to find the optimum performance of the synthesized nanocomposites, including: different pH of MO solution and different amount of nanocomposites (TiO₂/CNO-2, TiO₂/CNO-4, and TiO₂/CNO-6).

Characterization

Crystallinity and phase structure of the synthesized nanocomposites were studied using X-ray diffraction (XRD) patterns by Philips X'pert Pro MPD. Optical properties and optical band gap values were investigated for the different nanocomposites using diffuse reflectance spectroscopy (DRS) by Shimadzu UV-670 spectrophotometer. Composition and morphology of the synthesized nanocomposites were studied using field emission electron microscopy (FESEM) equipped with energy dispersive X-ray analyzer by

TESCAN mira 3. Photoluminescence (PL) analysis was carried out by Varian Cary Eclipse fluorescence spectrophotometer at excitation wavelength of 300 nm.

RESULTS AND DISCUSSION

XRD results

Fig. 1 shows the XRD patterns for the different synthesized samples, including pure TiO₂, Ni₂CuO₂, TiO₂/NCO-2, TiO₂/NCO-4, and TiO₂/NCO-6. As can be seen, the XRD pattern of the pure TiO, is consistent with diffraction planes corresponded to the anatase phase of TiO, (JCPDS file no.04-0477). The synthesized Ni₂CuO₃ nanoparticles represents the reflections which are matched with the orthorhombic phase of nickel copper oxide (JCPDS file. No 040-0959). As for the synthesized nanocomposites, the obtained patterns are consisted of both TiO₃ (marked with●) and Ni₂CuO₃ (marked with ⊗) phases. The diffraction peaks at $2\theta = 37.1^{\circ}$, 43.7° , and 61.9° are related to the Ni₂CuO₃ phase which are intensified with increasing the concentrations of the Ni₂CuO₃

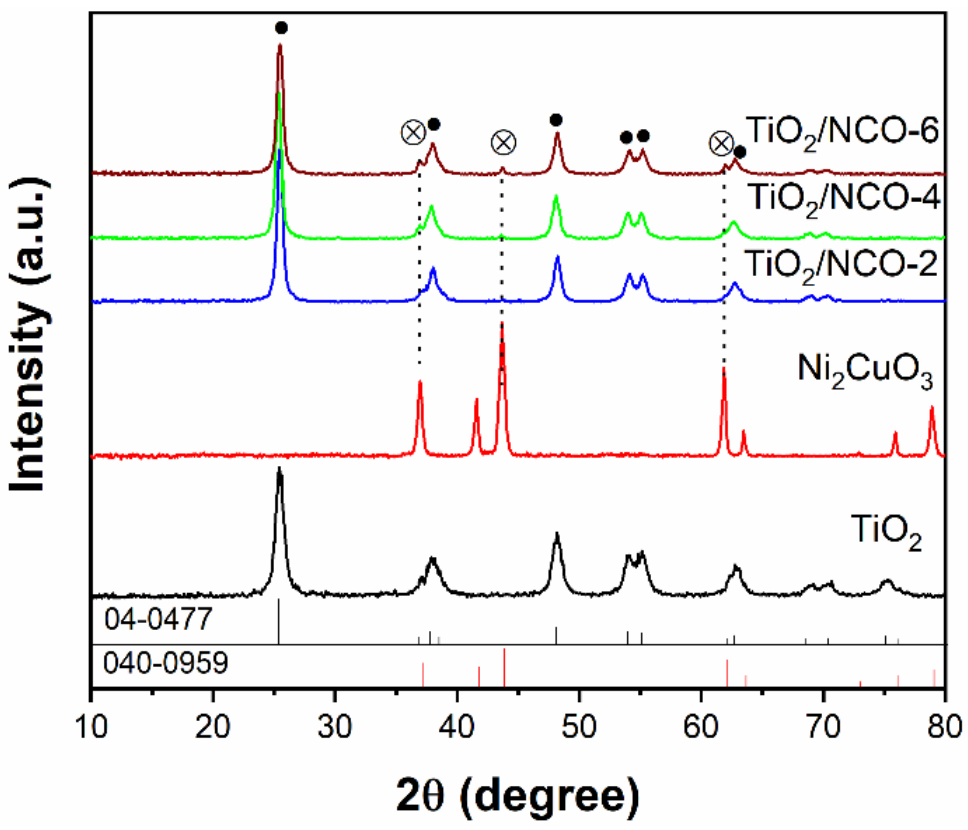


Fig. 1. XRD patterns of pure TiO₂, Ni₂CuO₃, TiO₂/NCO-2, TiO₂/NCO-4, and TiO₂/NCO-6.

within the nanocomposites.

DRS results

The DRS spectra for the pure ${\rm TiO_2}$, ${\rm TiO_2}/{\rm NCO}$ -2, ${\rm TiO_2}/{\rm NCO}$ -4, and ${\rm TiO_2}/{\rm NCO}$ -6 samples are provided in Fig. 2a. As seen, by increasing the concentration of ${\rm Ni_2CuO_3}$ phase in the nanocomposite to 4wt%, the light absorption in the visible light region increases. This observation can be attributed to the formation of new energy states, which effectively narrows the band gap of ${\rm TiO_2}$ [22]. The decreased band gap of the ${\rm TiO_2}/{\rm NCO}$ -4 nanocomposite favors for the visible-light harvesting, reflecting to the enhanced absorption in the range of 400

nm to 700 nm. However, more amount of the Ni₂CuO₃ (6 wt%) have no positive effect on the light absorption ability of the nanocomposite. For comparison, pure TiO₂ showed the weak light absorption in the visible light region.

Fig. 2b shows the $(\alpha hv)^2$ versus hv plots for the prepared samples. As expected, the $TiO_2/NCO-4$ nanocomposite possess lower band gap value of 2.65 eV, while pure TiO_2 , $TiO_2/NCO-2$, and $TiO_2/NCO-6$ have the band gaps of 3.46, 2.84, 2.76 eV, respectively.

PL results

Fig. 3 represents the PL spectra of the samples,

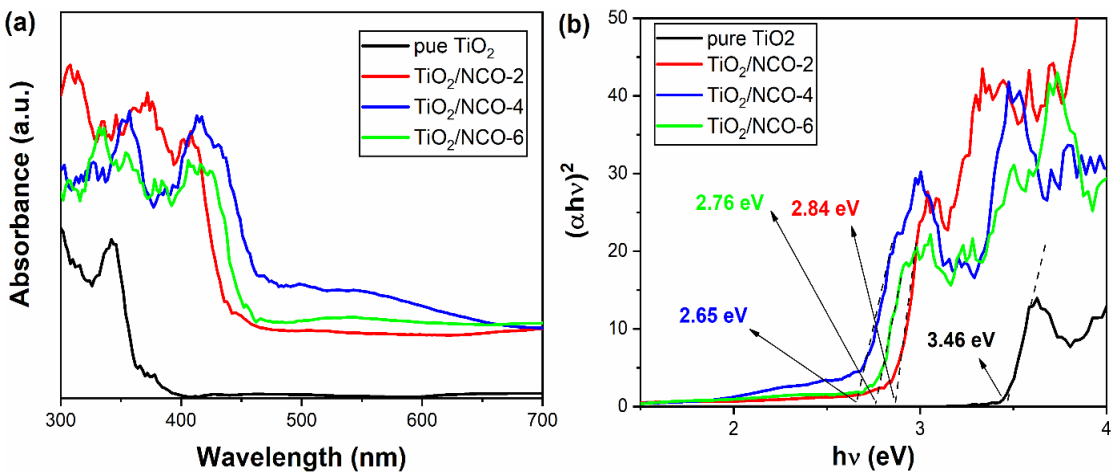


Fig. 2. DRD spectra (a) and Tauc plots (b) for the pure TiO₂/ TiO₂/NCO-2, TiO₂/NCO-4, and TiO₂/NCO-6.

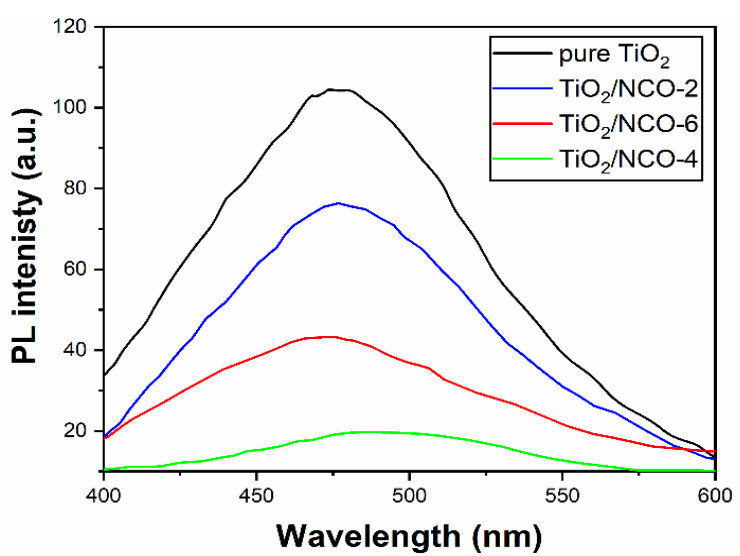


Fig. 3. PL spectra for the pure TiO₂, TiO₂/NCO-2, TiO₂/NCO-4, and TiO₂/NCO-6.

showing the lower PL intensity for the TiO₃/NCO-4 which reveals the decreased recombination rate of the charge carriers caused by addition of the Ni₂CuO₃ phase into TiO₃ structure. In agreement with the DRS results, the TiO₂/NCO-4 have the enhanced charge separation due the induced electron transitions between the energy states of the TiO₂ and Ni₂CuO₃ phases. Incorporation of 6wt% of the Ni₂CuO₃ into the nanocomposite caused to the increased recombination rate of the charges, highlighting in the slightly elevated PL intensity for the TiO₂/NCO-6 nanocomposite. Additionally, pure TiO, have the highest PL intensity, which implies that the photogenerated electrons and holes participate mainly to the radiative relaxation. These observations confirmed the efficient charge transitions between different energy levels of the incorporated TiO, and Ni₂CuO₃ nanoparticles [23,

24].

FESEM and EDX results

The FESEM image for the pure TiO, (Fig. 4a) shows the spherical nanoparticles in the size range below 100 nm. Due to the high surface energy of the nanoparticles, the agglomerated particles also are observed in the FESEM image [25]. Additionally, Fig. 4b exhibits the morphological properties of the TiO₂/NCO-4 nanocomposite. The very fine nanoparticles attached to the surface of the larger particles are observed, which can be attributed to the presence of Ni₂CuO₃ nanoparticles.

The EDX spectra for the pure TiO, and TiO,/NCO-4 are provided in Fig. 4c-d, respectively, verifying the presence of the constituents elements with their relative amounts given below: of Ti (51.22%), O (48.78%) for the pure TiO₂ sample; Ti (46.91%),

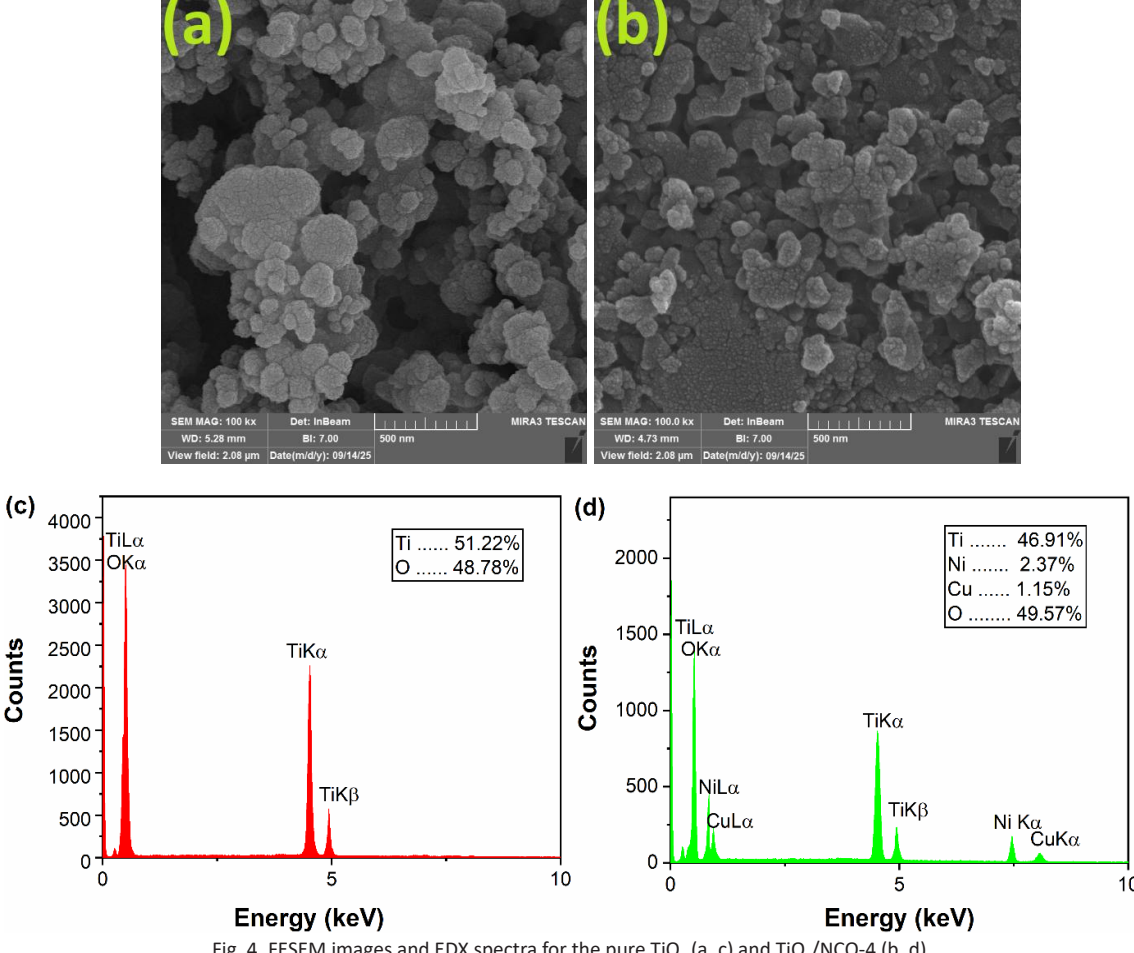


Fig. 4. FESEM images and EDX spectra for the pure TiO₂ (a, c) and TiO₂/NCO-4 (b, d).

Ni (2.37%), Cu (1.15%), and O (49.57%) for the $TiO_{\gamma}/NCO-4$ nanocomposite.

Photocatalysis results

The photocatalytic activity of the synthesized samples, including pure TiO₂, TiO₂/NCO-2, TiO₂/NCO-4, and TiO₂/NCO-6, was assessed for degradation of MO solution under visible light irradiation. Fig. 5 shows the degradation of MO solution under 150 min visible light illumination.

As seen, the TiO₂/NCO-4 nanocomposite exhibits the highest photoactivity about 94.17% for the degradation of MO solution. This observation is reasoned with the results of DRS and PL analyses, confirming the excellent photoactivity of the TiO₂/NCO-4 nanocomposite. The pure TiO₂, TiO₂/NCO-2, and TiO₂/NCO-6 showed the photocatalytic activities of the 27.48%, 51.14%, and 82.37%, respectively.

The effect of the different amounts of the loaded

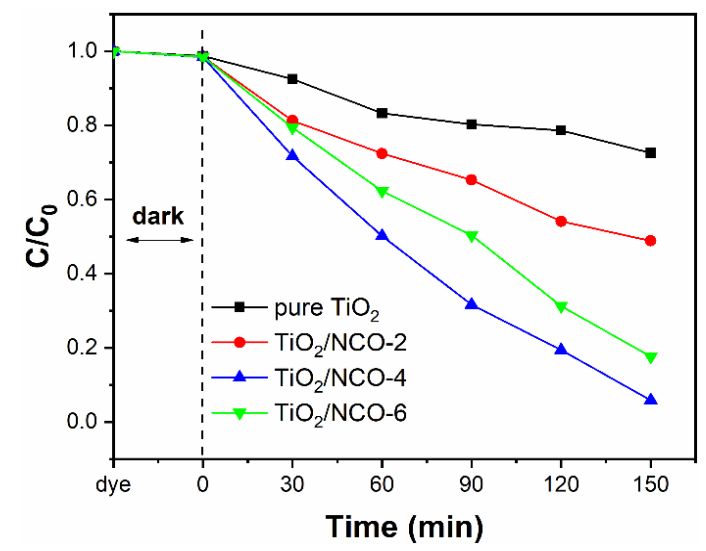


Fig. 5. Photocatalytic efficiency of the different ${\rm TiO_2/NCO}$ nanocomposites versus pure ${\rm TiO_3.}$

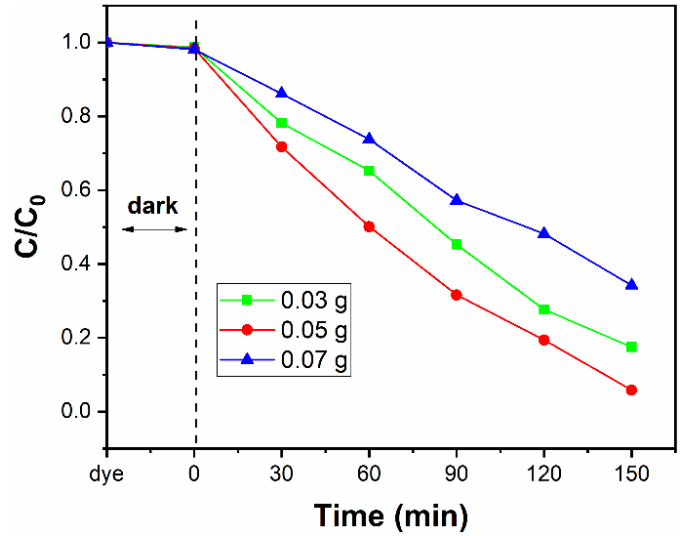


Fig. 6. Photocatalytic degradation of MO solution using different amounts of the TiO,/NCO-4 nanocomposite.

photocatalyst was studied for the TiO₂/NCO-4 nanocomposite. Fig. 6 shows that using more than 0.05 g of the TiO₂/NCO-4 nanocomposite lead to the decrease in the photocatalytic degradation of MO solution. This result can be attributed to the limitation of light beam to activate the photocatalyst in the turbid solution. The suspended photocatalyst particles, in exceeded amount, scatter the light beams, thereby limiting their penetration through the turbid solution [26, 27].

In addition, the effect of the different pH values of MO solution on the photocatalytic activity

of the ${\rm TiO}_2/{\rm NCO-4}$ nanocomposite was studied, provided in Fig. 7. Due to anionic nature of the MO dye [28, 29], the positively charged surface of the nanocomposite under acidic conditions facilitates the higher degradation level of the MO solution [30]. As seen from the Fig. 7, the photocatalytic activity of the MO solution increases to 99% by addition of HCl solution (0.5 M) until reaching the pH of 3. In contrast, under alkaline condition (pH = 9), the photocatalytic degradation of MO solution was dramatically decreased to 41.39%.

The reusability experiments were accomplished for the TiO₂/NCO-4 nanocomposite over 6

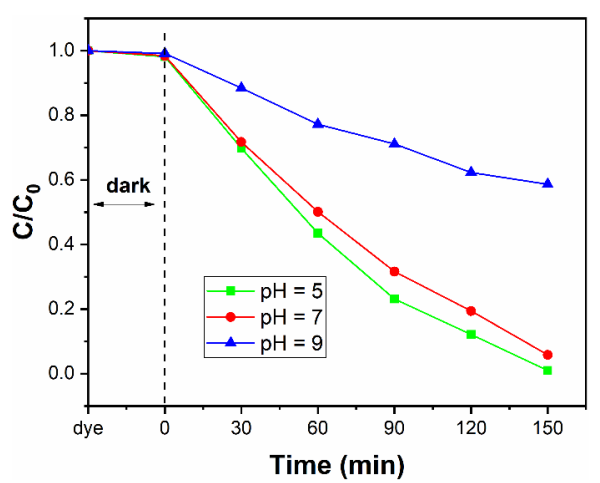


Fig. 7. Photocatalytic degradation of MO solution using TiO₂/NCO-4 at different pH conditions.

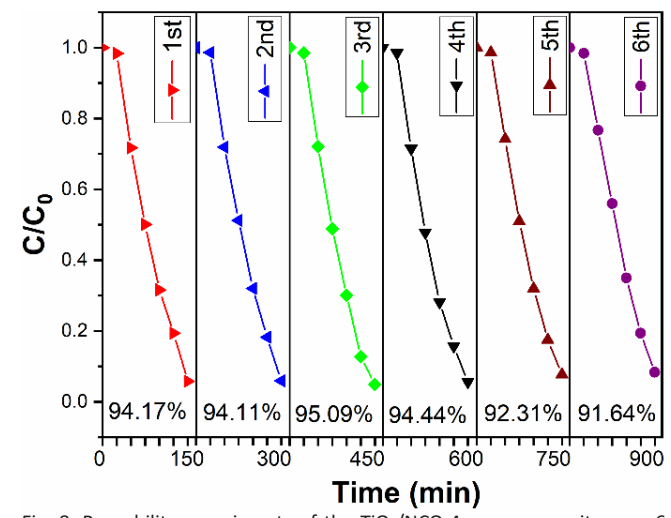


Fig. 8. Reusability experiments of the ${\rm TiO_2/NCO-4}$ nanocomposite over 6 reaction cycles.

successive reaction cycles. After each reaction cycle, the nanocomposite particles were separated using centrifugation at 700 rpm for 15 min, washed several times with distilled water, and then dried at 100 °C for 5 h. Fig. 8 exhibits the stability of the TiO₂/NCO-4 nanocomposite over 6 reaction cycles. The TiO₃/NCO-4 nanocomposite showed the excellent stability until 4th reaction cycles, without any significant decrement in the photocatalytic efficiency. But, after 5th and 6th reaction cycles, the decrease in the photocatalytic efficiency was 1.86% and 2.53%, respectively.

CONCLUSION

In summary, the synthesis TiO₃/ NCO nanocomposites containing different concentrations of Ni₂CuO₃ was reported as the efficient visible-light photocatalyst for degradation of organic dye. Using DRS and PL analyses, it was confirmed that the TiO₂/NCO-4 containing 4 wt% of the Ni₂CuO₃ has the lower optical band gap (2.65 eV), along with enhanced the visible-light absorption and improved the charge separation.

To assess the photocatalytic activity of the TiO₂/NCO nanocomposites, the visible light photocatalysis of the MO solution was performed under 150 min illumination. During this time, the TiO₂/NCO-4 showed the highest photocatalytic efficiency (94.17%) for removing of the MO solution. Conducting the photocatalytic reactions under different experimental conditions revealed that the optimal photocatalytic degradation was achieved with the 0.05 g of the TiO₃/NCO-4 nanocomposite in the acidic MO solution. Furthermore, the TiO₂/NCO-4 nanocomposite exhibited the appreciable stability over 6 consecutive reaction cycles.

CONFLICT OF INTEREST

The authors declare that there is no conflict of interests regarding the publication of this manuscript.

REFERENCES

- 1. Dunyo SK, Odei SA, Chaiwet W. Relationship between CO2 emissions, technological innovation, and energy intensity: Moderating effects of economic and political uncertainty. Journal of Cleaner Production, 2024:440:140904.
- 2. Zhou Y, Gu B. The impacts of human activities on Earth Critical Zone, Earth Critical Zone, 2024;1(1):100004.
- 3. Al Sharabati M, Abokwiek R, Al-Othman A, Tawalbeh M, Karaman C, Orooji Y, et al. Biodegradable polymers and their nano-composites for the removal of endocrine-disrupting chemicals (EDCs) from wastewater: A review. Environ Res.

2021;202:111694.

- 4. Mustafa FS, Oladipo AA. Rapid degradation of anionic azo dye from water using visible light-enabled binary metalorganic framework. Journal of Water Process Engineering. 2024:64:105686.
- 5. Hassani A, Krishnan S, Scaria J, Eghbali P, Nidheesh PV. Z-scheme photocatalysts for visible-light-driven pollutants degradation: A review on recent advancements. Curr Opin Solid State Mater Sci. 2021;25(5):100941.
- 6. Koe WS, Lee JW, Chong WC, Pang YL, Sim LC. An overview of photocatalytic degradation: photocatalysts, mechanisms, and development of photocatalytic membrane. Environmental Science and Pollution Research. 2019;27(3):2522-2565.
- 7. Liu S, Lou H, Luo J, Albashir D, Shi Y, Chen Q. A Novel In Situ Biosynthesized Bacterial Cellulose/MoS₂/TiO₂ Composite Film for Efficient Removal of Dyes and Pathogenic Bacteria from Industrial Wastewater under Sunlight Illumination. ACS Applied Materials & Interfaces. 2025;17(13):19543-19561.
- 8. Andreozzi R. Advanced oxidation processes (AOP) for water purification and recovery. Catal Today. 1999;53(1):51-59.
- 9. Ahmad I, Shukrullah S, Naz MY, Ahmed E, Ahmad M, Obaidullah AJ, et al. An aimed review of current advances, challenges, and future perspectives of TiO₂-based S-scheme heterojunction photocatalysts. Mater Sci Semicond Process. 2024;172:108088.
- 10. Morshedy AS, El-Fawal EM, Zaki T, El-Zahhar AA, Alghamdi MM, El Naggar AMA. A review on heterogeneous photocatalytic materials: Mechanism, perspectives, and environmental and energy sustainability applications. Inorg Chem Commun. 2024;163:112307.
- 11. Mustafa FS, Oladipo AA. Photocatalytic degradation of metronidazole and bacteria disinfection activity of Agdoped Ni_{0.5}Zn_{0.5}Fe₂O₄. Journal of Water Process Engineering. 2021:42:102132.
- 12. Abed SH, Shamkhi AF, Heydaryan K, Mohammadalizadeh M, Sajadi SM. Sol-gel Pechini preparation of CuEr2TiO6 nanoparticles as highly efficient photocatalyst for visible light degradation of acid red 88. Ceram Int. 2024;50(13):24096-24102.
- 13. Pelaez M, Nolan NT, Pillai SC, Seery MK, Falaras P, Kontos AG, et al. A review on the visible light active titanium dioxide photocatalysts for environmental applications. Applied Catalysis B: Environmental. 2012;125:331-349.
- 14. Cheng G, Liu X, Song X, Chen X, Dai W, Yuan R, et al. Visiblelight-driven deep oxidation of NO over Fe doped TiO2 catalyst: Synergic effect of Fe and oxygen vacancies. Applied Catalysis B: Environmental. 2020;277:119196.
- 15. Hernández-Alonso MD, Fresno F, Suárez S, Coronado JM. Development of alternative photocatalysts to TiO2: Challenges and opportunities. Energy and Environmental Science. 2009;2(12):1231.
- 16. Bessekhouad Y, Robert D, Weber JV. Bi₂S₃/TiO₂ and CdS/TiO, heterojunctions as an available configuration for photocatalytic degradation of organic pollutant. J Photochem Photobiol A: Chem. 2004;163(3):569-580.
- 17. Dozzi MV, Marzorati S, Longhi M, Coduri M, Artiglia L, Selli E. Photocatalytic activity of TiO₂-WO₃ mixed oxides in relation to electron transfer efficiency. Applied Catalysis B: Environmental. 2016;186:157-165.
- 18. Song KY, Park MK, Kwon YT, Lee HW, Chung WJ, Lee WI. Preparation of Transparent Particulate MoO₃/TiO₃ and

J Nanostruct 15(4): 2251-2259, Autumn 2025



- WO₃/TiO₂ Films and Their Photocatalytic Properties. Chem Mater. 2001;13(7):2349-2355.
- Rahbar M, Hosseini-Sarvari M. Natural sunlight-driven photocatalytic mineralization of petrochemical wastewater using ceramic-supported Fe, B co-doped TiO₂/CNT@WO₃ in a flat panel photoreactor. Journal of Water Process Engineering. 2025;77:108328.
- 20. Zhang X-x, Xiao Y-g, Cao S-s, Yin Z-l, Liu Z-Q. Ternary $TiO_2@Bi_2O_3@TiO_2$ hollow photocatalyst drives robust visible-light photocatalytic performance and excellent recyclability. Journal of Cleaner Production. 2022;352:131560.
- Kumar D, Sharma AR, Mishra YK, Sharma SK. Z-scheme CeO₂-TiO₂@CNT Heterojunction for Efficient Photoredox Removal of Mix Pollutants (CPF, MB, MO, and RhB). Small. 2024;21(5).
- 22. El-Yazeed WSA, Ahmed Al. Photocatalytic activity of mesoporous ${\rm WO_3/TiO_2}$ nanocomposites for the photodegradation of methylene blue. Inorg Chem Commun. 2019;105:102-111.
- 23. Zhang H, Chen G, Bahnemann DW. Photoelectrocatalytic materials for environmental applications. J Mater Chem. 2009;19(29):5089.
- Robert D. Photosensitization of TiO₂ by M_xO_γ and MxSy nanoparticles for heterogeneous photocatalysis applications. Catal Today. 2007;122(1-2):20-26.

- Jung SJ, Lutz T, Boese M, Holmes JD, Boland JJ. Surface Energy Driven Agglomeration and Growth of Single Crystal Metal Wires. Nano Lett. 2011;11(3):1294-1299.
- Mohammadi-Aghdam S, Mizwari ZM, Khojasteh H. Visible light photoactivity of the Cu doped TiO2/Yb2O3 nanocomposite for degradation of acid red 88 solution. J Sol-Gel Sci Technol. 2023;108(1):127-135.
- Sathish Kumar PS, Sivakumar R, Anandan S, Madhavan J, Maruthamuthu P, Ashokkumar M. Photocatalytic degradation of Acid Red 88 using Au–TiO₂ nanoparticles in aqueous solutions. Water Res. 2008;42(19):4878-4884.
- Usmanova GS, Latypova LR, Mustafin AG. Removal of Anionic Methyl Orange Dye from Water by Poly[2-methyl-1H-indole] Derivatives: Investigation of Kinetics and Isotherms of Adsorption. The Journal of Physical Chemistry B. 2024;128(17):4195-4207.
- 29. Subbaiah Munagapati V, Wen H-Y, Gollakota ARK, Wen J-C, Shu C-M, Andrew Lin K-Y, et al. Enhanced removal of anionic Methyl orange azo dye by an iron oxide (Fe₃O₄) loaded lotus leaf powder (LLP@Fe3O4) composite: Synthesis, characterization, kinetics, isotherms, and thermodynamic perspectives. Inorg Chem Commun. 2023;151:110625.
- 30. Wang J, Bai R. Formic acid enhanced effective degradation of methyl orange dye in aqueous solutions under UV–Vis irradiation. Water Res. 2016;101:103-113.